

AD-A062 248

NATIONAL BUREAU OF STANDARDS WASHINGTON DC SURFACE S--ETC F/G 7/3  
INFRARED SPECTRA OF CHEMISORBED CO ON RH.(U)  
NOV 78 J T YATES, T M DUNCAN, S D WORLEY

N00014-78-F-0008

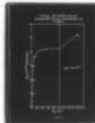
UNCLASSIFIED

TR-8

NI

|OF|

AD  
A062248



END

DATE  
FILMED

3--79

DDC

**LEVEL II**

OFFICE OF NAVAL RESEARCH  
Contract N00014-78-F-0008

12  
SC

AD A062248

Technical Report

Infrared Spectra of Chemisorbed CO on Rh

by

J. T. Yates, Jr.<sup>\*</sup>, T. M. Duncan, S. D. Worley<sup>†</sup>, and R. W. Vaughan

Department of Chemistry and Chemical Engineering  
California Institute of Technology  
Pasadena, California 91125

November 1, 1978

DDC  
RECEIVED  
DEC 14 1978  
F

DDC FILE COPY

Reproduction in whole or in part is permitted for  
any purpose of the United States Government

Approved for Public Release; Distribution Unlimited

To be published in the Journal of Chemical Physics

\* Sherman Fairchild Distinguished Scholar, on leave from the National Bureau of Standards, Washington, DC 20234.

† Visiting Guest Worker. Permanent address: Department of Chemistry, Auburn University, Auburn, Alabama 36830

78 12 11 061

UNCLASSIFIED

SECURITY CLASSIFICATION OF THIS PAGE (When Data Entered)

REPORT DOCUMENTATION PAGE		READ INSTRUCTIONS BEFORE COMPLETING FORM
1. REPORT NUMBER Technical Report No. 8 ✓	2. GOVT ACCESSION NO.	3. RECIPIENT'S CATALOG NUMBER
4. TITLE (and Subtitle) ⑥ Infrared Spectra of Chemisorbed CO on Rh		5. TYPE OF REPORT & PERIOD COVERED ⑨ Interim Repts
7. AUTHOR ⑩ J. T. Yates, Jr., T. M. Duncan, S. D. Worley and R. W. Vaughan		6. PERFORMING ORG. REPORT NUMBER
9. PERFORMING ORGANIZATION NAME AND ADDRESS Surface Science Division National Bureau of Standards Washington, DC 20234		8. CONTRACT OR GRANT NUMBER(s) ⑮ NO0014-78-F-0008 NO0014-75-C-0960
11. CONTROLLING OFFICE NAME AND ADDRESS Office of Naval Research Physical Program Office Arlington, VA 22217		10. PROGRAM ELEMENT, PROJECT, TASK AREA & WORK UNIT NUMBERS
14. MONITORING AGENCY NAME & ADDRESS (if different from Controlling Office)		12. REPORT DATE Nov. 1, 1978
		13. NUMBER OF PAGES 28
		15. SECURITY CLASS. (of this report) Unclassified
		15a. DECLASSIFICATION/DOWNGRADING SCHEDULE
16. DISTRIBUTION STATEMENT (of this Report) Approved for Public Release; Distribution Unlimited. ⑪ 1 Nov 78 ⑫ 32 p		
17. DISTRIBUTION STATEMENT (of the abstract entered in Block 20, if different from Report) ⑭ TR-8		
18. SUPPLEMENTARY NOTES Preprint; to be published in Journal of Chemical Physics.		
19. KEY WORDS (Continue on reverse side if necessary and identify by block number) Adsorbate structure; isotopic shifts; desorption; infrared spectra; isotopic exchange; rhodium.		
20. ABSTRACT (Continue on reverse side if necessary and identify by block number) The infrared spectrum of CO chemisorbed on alumina-supported Rh atoms has been investigated. In agreement with previous work, three types of adsorbed species have been clearly distinguished on the basis of their C-O stretching frequencies. Species I, assigned as Rh(CO) <sub>2</sub> , is formed only with Rh atoms which are isolated from each other. Species II, assigned as Rh-CO, and III, assigned as Rh <sub>2</sub> CO, are formed on Rh clusters having two or more Rh atoms. CO-species II and III undergo interactions with neighbor CO species causing an (Continued on reverse side)		

DD FORM 1 JAN 73 1473

EDITION OF 1 NOV 65 IS OBSOLETE  
S/N 0102-014-6601

UNCLASSIFIED

SECURITY CLASSIFICATION OF THIS PAGE (When Data Entered)


410 655



UNCLASSIFIED

SECURITY CLASSIFICATION OF THIS PAGE(When Data Entered)

increase in wavenumber as coverage increases. Based on infrared intensity measurements for species I, the OC-Rh-CO angle is  $90^\circ$ . Chemisorbed  $^{13}\text{CO}$  yields the expected infrared spectrum on Rh, and rapid isotopic exchange between  $^{13}\text{CO(ads)}$  and  $^{12}\text{CO(g)}$  is observed which cannot be explained by the observed rate of desorption of CO from the supported Rh surface.

ACCESSION for	
NTIS	Wide Section <input checked="" type="checkbox"/>
DDC	B II Section <input type="checkbox"/>
UNANNOUNCED	<input type="checkbox"/>
JUSTIFICATION	
BY	
DISTRIBUTION/AVAILABILITY NOTES	
DI	
	

UNCLASSIFIED

SECURITY CLASSIFICATION OF THIS PAGE(When Data Entered)



INFRARED SPECTRA OF CHEMISORBED CO ON Rh

J. T. Yates, Jr.<sup>\*</sup>, T. M. Duncan, S. D. Worley<sup>†</sup>, and R. W. Vaughan

Department of Chemistry and Chemical Engineering  
California Institute of Technology  
Pasadena, California 91125

\* Sherman Fairchild Distinguished Scholar, on leave from NBS, Washington, D.C. 20234. To whom all correspondence should be addressed.

† Visiting guest-worker. Permanent address: Department of Chemistry, Auburn University, Auburn, Alabama 36830.

### Abstract

The infrared spectrum of CO chemisorbed on alumina-supported Rh atoms has been investigated. In agreement with previous work, three types of adsorbed species have been clearly distinguished on the basis of their C-O stretching frequencies. Species I, assigned as  $\text{Rh}(\text{CO})_2$ , is formed only with Rh atoms which are isolated from each other. Species II, assigned as  $\text{Rh}-\text{CO}$ , and III, assigned as  $\text{Rh}_2\text{CO}$ , are formed on Rh clusters having two or more Rh atoms. CO-species II and III undergo interactions with neighbor CO species causing an increase in wavenumber as coverage increases. Based on infrared intensity measurements for species I, the OC-Rh-CO angle is  $\sim 90^\circ$ . Chemisorbed  $^{13}\text{C}$ O yields the expected infrared spectrum on Rh, and rapid isotopic exchange between  $^{13}\text{C}(\text{ads})$  and  $^{12}\text{C}(\text{g})$  is observed which cannot be explained by the observed rate of desorption of CO from the supported Rh surface.



## I. INTRODUCTION

The chemisorption of CO on transition metals has been studied by many physical techniques in an effort to understand the molecular and electronic character of the adsorbed species. The surface measurement techniques at our disposal range from those useful for studying adsorbed layers on single crystal surfaces to other techniques which may be more readily applied to metal adsorbents which are highly dispersed on inert, high area, supports. It is the latter class of surfaces which more closely resemble heterogeneous catalysts used in practice, and in fact the ability to disperse precious metals has been of major importance in enhancing their usefulness as catalysts.

While the study of single crystal adsorbents represents a limit of refinement in one direction (e.g., high-purity substrates, well-defined atomic periodicity and electronic character, etc.), dispersed metal catalysts can in principle achieve a limiting case in the opposite direction (atomic dispersal to the limit of single isolated metal atoms). Comparisons between chemisorbed CO on single metal atoms (or small metal clusters) and the vast literature of metal carbonyl chemistry have often been made<sup>(1,2)</sup>. Such comparisons are often extended to single crystals containing chemisorbed CO<sup>(2,3)</sup>.

One of the best ways to study the structure of chemisorbed species involves the use of vibrational spectroscopy. This has been effectively carried out on single crystals using electron energy loss spectroscopy (EELS)<sup>(3-6)</sup> as well as reflection-absorption infrared spectroscopy (RAIS)<sup>(7-9)</sup>. On dispersed metals, inelastic electron tunneling spectroscopy (IETS) has recently been employed<sup>(10)</sup>. However, most vibrational work to date on dispersed metals has been done using transmission infrared spectroscopy<sup>(11,12)</sup>. For both single crystals and dispersed metals, the infrared techniques currently offer the highest frequency resolution, and this technique is therefore more suitable for



work involving isotopic labeling where small spectral shifts may be involved.

The chemisorption of CO by supported Rh has been well studied in the past, using infrared spectroscopy. For  $\text{Al}_2\text{O}_3$ -supported Rh, Yang and Garland<sup>(13)</sup> first postulated that at low Rh concentrations, where sintering did not occur at reduction temperatures below  $200^\circ\text{C}$ , Rh existed in a condition closely approaching atomic dispersion (i.e. isolated Rh atoms). This picture has been confirmed by others on  $\text{Al}_2\text{O}_3$ <sup>(14-17)</sup> although there are differences in interpretation regarding the degree of dispersion. Yao and Rothschild<sup>(17)</sup> regard the Rh as existing as isolated atoms on  $\text{Al}_2\text{O}_3$  at 0.9 wt.% Rh on  $\gamma\text{-Al}_2\text{O}_3$ . D. J. C. Yates<sup>(16)</sup> regards the Rh to exist as tiny "rafts," containing about 7 atoms, with 6 atoms being edge atoms and behaving as if they are isolated. It has been shown in several laboratories that these highly dispersed Rh atoms are able to adsorb 2 CO molecules each, yielding a doublet in the infrared spectrum corresponding to symmetric and antisymmetric coupling between pairs of CO molecules adsorbed on the same Rh atom<sup>(13-17)</sup>. The close correspondence between the doublet frequencies and the spectrum of  $\text{Rh}_2(\text{CO})_4\text{Cl}_2$  and  $\text{Rh}_2(\text{CO})_4\text{Br}_2$  (which contain pairs of linear CO molecules on each Rh atom<sup>(13,18,19)</sup>) leaves little doubt regarding this assignment.

In this paper, we reinvestigate the CO/Rh system using infrared spectroscopy, volumetric uptake and isotopic substitution.

## II. EXPERIMENTAL

The infrared cell used in these experiments is shown in Figure 1. It consists of two stainless steel "conflat" flanges containing 33 mm diameter  $\text{CaF}_2$  single crystal windows which are sealed to a Ag ring using AgCl cement. Such windows are commercially available<sup>(20)</sup>. The cell may be assembled using

Cu gaskets and a double-sided flange which serves as the central section of the cell.

The vacuum system used in this work is a small bakeable all-metal system capable of being pumped below  $10^{-8}$  torr with a  $20 \text{ l sec}^{-1}$  ion pump. In addition, for handling higher pressure gases, the system may be evacuated with a  $\text{l-N}_2$  trapped forepump. Pressure may be measured with a bakeable Baratron capacitance monometer to  $\pm 0.001$  torr. A Bayard-Alpert gauge is used for background pressure measurements below  $10^{-4}$  torr.

The Rh samples are supported on  $\text{Al}_2\text{O}_3$ <sup>(21)</sup> and are prepared as described by Yang and Garland<sup>(13)</sup>. Briefly, an aqueous solution of  $\text{RhCl}_3$  is diluted 10:1 with reagent-grade acetone and high-area  $\text{Al}_2\text{O}_3$  is added with stirring. This slurry is continuously mixed while being sprayed with an atomizer onto the  $\text{CaF}_2$  window maintained at  $80^\circ \text{C}$ . Flash evaporation of the solvent during spraying leaves an adherent coating on the window. The weight of these deposits is  $\sim 11 \text{ mg/cm}^2$  and the Rh content is 2.2% by weight. The cell is then assembled and the deposit is degassed by pumping at room temperature. Following this, the deposit and the cell are heated in a circulating-air oven to  $150^\circ \text{C}$  for 4 hours while degassing with the ion pump. Reduction to Rh metal is achieved using  $\text{H}_2(\text{g})$  (Matheson grade 99.9995% pure) which has been stored at 1.3 atmospheres in a stainless steel tube immersed in  $\text{l-N}_2$ . Three sequential  $400 \text{ cm}^3$  charges of  $\text{H}_2$  at  $\sim 180$  torr are used during reduction at  $150^\circ \text{C}$ , with the final reduction being carried out for 1 hour. Following reduction, the  $\text{Rh/Al}_2\text{O}_3$  is outgassed at  $175^\circ \text{C}$  for  $\sim 8$  hours until the background pressure falls below  $1 \times 10^{-6}$  torr. Following cooling, a background IR spectrum from  $4000 \text{ cm}^{-1}$  to  $1000 \text{ cm}^{-1}$  is recorded. The sample is then ready for adsorption experiments. All spectra reported have been obtained by subtraction of the smooth background.



The infrared spectrometer is a Perkin-Elmer Model 180 grating spectrometer operated in the  $2000\text{ cm}^{-1}$  region with a spectral resolution of  $2.6\text{ cm}^{-1}$ . Spectra are recorded in the absorbance mode using the double beam facility. Calibration of the instrument's absorbance scale is carried out using standard density grids. The wavenumber scale was calibrated<sup>(22)</sup> above  $2000\text{ cm}^{-1}$  with a gas cell containing CO(g) at  $\sim 150$  torr. Below  $2000\text{ cm}^{-1}$  the Q-branch of  $\text{H}_2\text{CO(g)}$  at  $1750\text{ cm}^{-1}$ <sup>(23)</sup> was used as a calibration point. A  $5\text{ cm}^{-1}$  shift in the two scales occurs at  $2000\text{ cm}^{-1}$  due to a grating change in the spectrometer. The reported spectral features in this paper are accurate to  $1\text{ cm}^{-1}$ .

Spectroscopic grade CO from a glass breakseal bulb was used for adsorption without further purification.  $^{13}\text{CO}$  was obtained from Merck Isotopes at 90% enrichment and was used without purification.

### III. RESULTS

#### A. Adsorption Isotherm

By means of pressure measurements in the vacuum system of known volume, it was possible to measure accurately the number of CO molecules adsorbed by the Rh samples. A plot of typical results is shown in Figure 2. It was found that the final equilibrium pressure was approached very slowly in these measurements so that small positive errors in the pressure corresponding to each point may exist. This does not affect the measurement of the quantity of CO adsorbed. Beyond an equilibrium pressure of  $\sim 1$  torr, errors due to volumetric and pressure uncertainties become too great for accurate continuation of the isotherm. The points (a) to (e) on the isotherm in Figure 2 correspond to the labeled infrared spectra in Figure 3. It was found that the integrated IR intensity in spectra (a) to (e) increased in a linear fashion with the number of CO molecules chemisorbed. Thus, assuming this relationship to hold



for the entire range of coverage, we may calculate the approximate number of CO molecules adsorbed per Rh atom at high CO pressures from the integrated intensity of the spectra. At a final  $P_{CO} = 50$  torr,  $\frac{N_{CO}}{N_{Rh}} = 0.92$  using this method.

### B. Infrared Spectra of $^{12}CO$ Adsorbed on Rh

Following each adsorption point in Figure 2, the infrared spectra shown in Figure 3 were recorded. Four spectral features are clearly evident at all coverages of CO. A broad band at  $1855\text{ cm}^{-1}$  develops and shifts to  $1870\text{ cm}^{-1}$  as coverage increases. This band is assigned to CO bonded to more than one Rh atom and is termed "bridged-CO,"  $Rh_2(CO)^{(13)}$ . A second band of low relative intensity is observed at  $2056\text{ cm}^{-1}$  at lowest CO coverage and shifts upward to  $2070\text{ cm}^{-1}$  as coverage increases. This is assigned as a linear-CO species bonded to a single Rh atom which exists in coordination with other Rh atoms,  $Rh(CO)^{(13)}$ . It has been shown previously that as the concentration of Rh on the  $Al_2O_3$  support is increased, both the linear and bridged-CO species are enhanced in relative intensity<sup>(13)</sup>. The most pronounced spectral feature in Figure 3 is a doublet with components at  $2101\text{ cm}^{-1}$  and  $2031\text{ cm}^{-1}$ . This doublet increases in intensity during the entire course of adsorption without change in wavenumber, as reported previously by Yang and Garland<sup>(13)</sup>. The doublet is assigned to a pair of CO molecules adsorbed on isolated Rh atoms,  $Rh(CO)_2^{(13)}$ . Spectrum (g) of Figure 1 was taken with  $\sim 50$  torr  $^{12}CO$  above the Rh surface, and on the leading edge of the highest wavenumber peak one can see the fine structure of the  $CO(g)$  superimposed on the spectrum. These spectra correspond almost exactly to those obtained by Yang and Garland<sup>(13)</sup>, except that a bridged-CO bond was not observed in their work on 2% Rh samples prepared in similar fashion to ours.

Comparisons with the literature are summarized below in Table I.

### C. Desorption of $^{12}\text{CO}$ from Rh

It was found that CO could be reversibly desorbed thermally at  $T \leq 336$  K. Representative spectra are shown in Figure 4 for desorption. It was found that rapid desorption occurs initially at 295 K for the  $\text{Rh}(\text{CO})_2$  species and that both  $\text{Rh}_2(\text{CO})$  and  $\text{Rh}(\text{CO})$  species appear to desorb less rapidly than  $\text{Rh}(\text{CO})_2$ , as reported by others<sup>(13,17)</sup>. However, at 295 K the rate of loss of infrared intensity decreases significantly following the first desorption stage, and the surface must be warmed slightly to promote more rapid removal of chemisorbed CO.

It should be noted that the wavenumber of the components of the  $\text{Rh}(\text{CO})_2$  doublet is invariant at all stages of desorption whereas both the  $\text{Rh}(\text{CO})$  and  $\text{Rh}_2(\text{CO})$  features shift to slightly lower wavenumber as desorption progresses.

Following spectrum (d), CO was readsorbed at ~50 torr and spectrum (a) was reproduced almost exactly. The reversible behavior for CO adsorption and desorption below 336 K suggests that CO dissociation (or disproportionation), leaving a carbon residue on the surface, does not occur below 336 K. Carbonization of bulk Rh by CO has been reported at 573 K<sup>(24)</sup>.

### D. Infrared Spectrum of $^{13}\text{CO}$ Adsorbed on Rh

Adsorption experiments were repeated on a freshly prepared  $\text{Rh}/\text{Al}_2\text{O}_3$  surface using 90%  $^{13}\text{CO}$  as the adsorbate. The spectra for increasing exposure to CO are shown in Figure 5. The general behavior observed for  $^{12}\text{CO}$  is reproduced for  $^{13}\text{CO}$ , and a comparison of wavenumbers for each isotopic species is given in Table II. An unusual and reproducible effect may be seen in comparison of  $^{12}\text{CO}$  spectra and  $^{13}\text{CO}$  spectra (Figures 3 and 5). The intensities for the two components of the doublet invert when the different CO isotopes are adsorbed.



### E. Infrared Spectrum of Rh(<sup>13</sup>CO)(<sup>12</sup>CO)

Since the <sup>13</sup>CO used above contains 10% <sup>12</sup>CO, a doublet feature due to Rh(<sup>13</sup>CO)(<sup>12</sup>CO) is expected. The high wavenumber component of this doublet is seen in Figure 5 at 2036 cm<sup>-1</sup>. The low wavenumber component is unfortunately hidden under the <sup>13</sup>CO features near 2000 cm<sup>-1</sup>. The statistical fraction, X, of Rh(<sup>13</sup>CO)(<sup>12</sup>CO) on this surface is 0.09. Using the maximum absorbance peak heights, A, for the two high wavenumber bands, we see that the ratio of absorbances, R<sub>A</sub> is

$$R_A = \frac{A_{12,13}}{A_{12,12} + A_{12,13} + A_{13,13}} = \frac{0.1}{0.01 + 0.1 + 0.93} = 0.096 \sim X \quad (1)$$

where A<sub>12,12</sub> was not measured but assumed to be 0.01 from the statistics of mixing.

### F. Exchange of <sup>13</sup>CO(ads) with <sup>12</sup>CO(g)

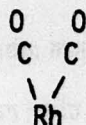
Following the observation of the spectrum for <sup>13</sup>CO in Figure 4, 50 torr of <sup>12</sup>CO(g) was introduced into the infrared cell, and the spectrum shown in Figure 6 was measured within 11 minutes. Almost complete exchange of all isotopic CO-adsorbed species was observed in this short time, and the rapidity of this exchange process sharply contrasts with the slow rate of desorption observed in Figure 4. In addition, following exchange, a shoulder due to the low-frequency component of the Rh(<sup>13</sup>CO)(<sup>12</sup>CO) doublet is now seen near ~2012 cm<sup>-1</sup>. Unfortunately, it is not possible to determine the exact frequency of the Rh(<sup>13</sup>CO)(<sup>12</sup>CO) low wavenumber component because the shoulder at ~2012 cm<sup>-1</sup> contains contributions from an unknown ratio of Rh(<sup>13</sup>CO)<sub>2</sub>, Rh(<sup>13</sup>CO)(<sup>12</sup>CO), and Rh(<sup>12</sup>CO)<sub>2</sub>.



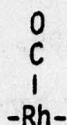
#### IV. DISCUSSION

##### A. Assignment of IR Spectral Features

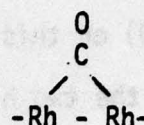
Three infrared-active adsorbed species are clearly seen from the spectra of chemisorbed CO on Rh. They are:



I



II



III

The assignment of species I is made on the basis of the doublet in the infrared spectrum and its close correspondence with the spectrum of  $\text{Rh}_2(\text{CO})_4\text{X}_2$  where  $\text{X} = \text{Cl}$  or  $\text{Br}$ <sup>(19)</sup>. This comparison is tabulated in Table III and was originally proposed by Yang and Garland<sup>(13)</sup> as evidence for species I.

The striking feature to be noted regarding the infrared spectrum of species I is that both the CO stretching frequencies are invariant to within  $1 \text{ cm}^{-1}$  over the entire coverage range studied here (a 30-fold range of infrared intensity). This may be regarded as strongly indicative that the Rh atoms associated with species I are in fact isolated Rh atoms on the  $\text{Al}_2\text{O}_3$  support. For Rh atoms within a Rh cluster, CO adsorption on neighboring Rh atoms should lead to interactions producing an increase in wavenumber as CO coverage increases. This behavior is generally observed for interacting CO molecules on bulk metals and may lead at full CO coverage to shifts of  $\sim 100 \text{ cm}^{-1}$  in the C-O vibration. It is now generally accepted that interactional effects between CO molecules can occur via three mechanisms, namely dipole-dipole coupling, direct intermolecular repulsion, and indirect effects through the metal<sup>(9,3)</sup>. The suggestion that the lack of a coverage-dependent shift for species I was

indicative of isolated Rh atoms was first made by Yang and Garland<sup>(13)</sup>. This view is confirmed by Yao and Rothschild<sup>(17)</sup>, who suggest that on their Rh/Al<sub>2</sub>O<sub>3</sub> surface Rh...Rh distances of order 8 Å are necessary for Rh(CO)<sub>2</sub> formation. The results of this study are in agreement with this general view that isolated Rh atoms are present.

Both species II and III are associated with infrared bands which shift upwards by ~15 cm<sup>-1</sup> as CO coverage rises to saturation. These bands also exhibit reversible wavenumber behavior upon desorption. On this basis, both species are thought to exist on Rh sites which are coordinated to other Rh atoms. The first site of this type would be Rh<sub>2</sub>. Multiple Rh coordination would permit interactional effects between neighbor CO molecules on neighbor Rh atoms.

#### B. Estimate of the Fraction of Rh Present as Isolated Atoms

A qualitative model involving only Rh and Rh<sub>x</sub> sites is presented in this section. In this model we assume that all Rh<sub>x</sub> sites adsorb only the bridged-CO species, III. The amount of species II is assumed to be zero in conformance with the low intensity associated with this species (Figures 2-4).

Let  $N_s$  = number of single Rh atoms.

$N_B$  = number of Rh<sub>x</sub> sites.

Then,

$$N_s + xN_B = N_{Rh}$$

$$2N_s + N_B = N_{CO}$$

From our volumetric uptake and infrared measurements,  $N_{CO}/N_{Rh} = 0.92$  at saturation. For  $x = 2$ ,  $N_s/N_B = 0.8$ . For  $x = 3$ ,  $N_s/N_B = 1.62$ . These ratios correspond to ~40% or ~60% isolated Rh atom sites, respectively. A comparison of the integrated intensity of the doublet feature to the integrated intensity of the



bridged-CO feature indicates that ~60% of the total integrated intensity is within the doublet feature. Based on the assumption of equivalent extinction coefficients per CO moiety for the two structures I and III, this measurement would suggest that ~30% of the sites are isolated Rh atom sites. While these two methods of calculation both suffer from the approximations made, it is clear that an appreciable fraction of the adsorption sites (30-60%) is capable of adsorbing 2-CO molecules and should be considered as isolated Rh atoms.

### C. Carbonyl Bonding in Rh(CO)<sub>2</sub>

The high wavenumber component in the doublet feature of Rh(CO)<sub>2</sub> corresponds to the symmetric CO-stretching mode and is assigned in this fashion in metal carbonyl spectra<sup>(26-28)</sup>. The low wavenumber component is the result of antisymmetric coupling between CO oscillators. It has been demonstrated in metal carbonyls<sup>(27)</sup> that the ratio of integrated absorbance, ( $A_{\text{asym}}/A_{\text{sym}}$ ), is related to the angle, ( $2\alpha$ ), between carbonyl groups as follows:

$$\frac{A_{\text{asym}}}{A_{\text{sym}}} = \tan^2 \alpha \quad (2)$$

As an example of the application of this equation, in the compound  $(\pi\text{-C}_5\text{H}_5)\text{Fe(CO)}_2\text{Sn(Ph)}_3$ , the measured intensity ratio gives a value of  $2\alpha = 93^\circ$  whereas x-ray studies give  $2\alpha = 95^\circ$ <sup>(28)</sup>.

Because of overlap with other bands in Figure 2, it is not possible from our data to measure accurately  $A_{\text{asym}}/A_{\text{sym}}$ . However, from other work<sup>(17)</sup> where because of higher Rh dispersion this overlap was virtually eliminated,  $A_{\text{asym}}/A_{\text{sym}} \approx 1.0$ , yielding  $2\alpha \approx 90^\circ$ . This is in good agreement with the bond angle ( $91^\circ$ ) between carbonyl groups in  $\text{Rh}_2(\text{CO})_4\text{Cl}_2$ <sup>(18)</sup> and with the ratio  $(A_{\text{asym}}/A_{\text{sym}}) = 1.0 \pm 0.1$  measured for this compound<sup>(13)</sup>. On this basis, we



conclude that the bond angle between CO's is near  $90^\circ$  for  $\text{Rh}(\text{CO})_2$ .

#### D. Isotopic Shift for $^{13}\text{C}$ O-Labeled Species

For completely labeled carbonyl species, the isotopic wavenumber ratio is given by

$$\frac{\nu}{\nu^*} = \left( \frac{\mu_{\text{CO}}}{\mu_{\text{CO}}^*} \right)^{1/2} \quad (3)$$

where  $\mu_{\text{CO}}$  or  $\mu_{\text{CO}}^*$  are the reduced masses of the unlabeled and labeled CO molecule<sup>(26)</sup>. In Table II, the observed wavenumbers and their isotopic shifts are shown from our experimental measurements and from the calculation based on Equation (3). All wavenumber shifts calculated are in agreement with measured shifts within the experimental error of locating band centers.

An explanation for the intensity inversion of the symmetric and anti-symmetric bands for species I following  $^{13}\text{C}$ O isotopic substitution is currently under investigation.

#### E. Comparison of Isotopic Exchange with Desorption Measurements

All of the adsorbed CO species, I, II, and III, undergo rapid isotopic exchange with CO(g) at 295 K, as shown in Figure 6. It was noted that the exchange of  $^{13}\text{C}(\text{ads})$  with  $^{12}\text{C}(\text{g})$  at 50 torr was much faster than the CO desorption rate (Figure 4) in vacuum at 295 K.

Two possible explanations can be offered to explain the rapidity and completeness of CO exchange at high CO pressures:

1. High pressure CO above a surface containing species I, II, and III is able to produce transient adsorbed species containing extra CO moieties. Isotopic exchange with CO(g) takes place readily via these intermediate species.

2. A fraction of the Rh and  $Rh_x$  sites is buried in pores within the support and is rapidly accessible only at high CO pressures. Because of readsorption processes during desorption from these buried sites, the rate of desorption is slow. However, at high CO pressures (~50 torr) both adsorption and isotopic exchange occur readily.

We believe that both explanations may be involved here. The rapidity and completeness of exchange suggests that model (1) above is operative. The very great decrease observed for the desorption rate of spectroscopically similar CO (i.e., species I) suggests that model (2) applies to a fraction of the Rh on the supported surface.

#### V. SUMMARY

The following features of CO adsorption on  $Rh/Al_2O_3$  have been determined or verified:

1. Three CO species, I, II, and III, are distinguishable on  $Rh/Al_2O_3$  surfaces.
2. Species I,  $Rh(CO)_2$ , is produced on isolated Rh atoms as judged from lack of evidence for interaction with neighboring CO molecules as coverage is increased.
3. Species II and III are able to undergo interaction with neighboring CO molecules adsorbed on neighbor Rh atoms. This suggests the presence of some  $Rh_x$  species.
4. An estimate of a surface population of 30-60% isolated Rh atom sites is made, based on spectral band development and volumetric uptake measurements.
5. Species I exists with an angle  $\sim 90^\circ$  between CO groups.



6.  $^{13}\text{CO}$  substitution for  $^{12}\text{CO}$  yields the expected isotopic shifts.
7. One feature in the spectrum of  $\text{Rh}(^{12}\text{CO})(^{13}\text{CO})$  has been observed at  $2086\text{ cm}^{-1}$ , lending further confirmation to the structure postulated for species I.
8. Rapid isotopic exchange of  $^{12}\text{CO}$  with  $^{13}\text{CO}(\text{ads})$  occurs for all of the adsorbed CO species. This suggests the existence of transient adsorbed species containing more CO moieties than species I, II, and III.

#### VI. ACKNOWLEDGMENT

The authors gratefully acknowledge support from ONR under contract N00014-77-F-0008 and N00014-75-C-0960. We also acknowledge valuable discussions with Dr. Ben Huie. We thank Professor George F. Rossman for his kindness in allowing us to use the infrared spectrometer.

### References

1. T. L. Brown and D. J. Darensbourg, *Inorg. Chem.* **6**, 971 (1967).  
R. P. Eischens, S. A. Francis, and W. A. Pliskin, *J. Phys. Chem.* **60**, 194 (1956); G. Blyholder, *J. Phys. Chem.* **68**, 2772 (1968).
2. H. Conrad, G. Ertl, H. Knözinger, J. Küppers and E. E. Latta, *Chem. Phys. Lett.* **42**, 115 (1976).
3. G. E. Thomas and W. H. Weinberg, submitted, *J. Chem. Phys.*
4. H. Ibach, M. Hopster, and B. Sexton, *Application of Surface Science* **1**, 1 (1977).
5. G. Dalmai-Imelik, J. C. Bertolini, and J. Rousseau, *Surface Science* **63**, 67 (1977).
6. S. Andersson, *Solid State Comm.* **20**, 229 (1976); **21**, 75 (1977).
7. J. Pritchard, M. L. Sims, *Trans. Far. Soc.* **66**, 427 (1970); J. Pritchard, T. Catterick, and R. K. Gupta, *Sur. Sci.* **53**, 1 (1975).
8. J. T. Yates, Jr. and D. A. King, *Surface Sci.* **30**, 601 (1972); J. T. Yates, Jr., R. G. Greenler, I. Rataczykowa, and D. A. King, *Surface Sci.* **36**, 739 (1973).
9. A. M. Bradshaw and F. M. Hoffman, *Surface Sci.* **72**, 513 (1978).
10. P. K. Hansma, W. C. Koska, and R. M. Laire, *J. Amer. Chem. Soc.* **98**, 6064 (1976).
11. L. H. Little, *Infrared Spectra of Adsorbed Species* (Academic Press, London, 1966).
12. M. L. Hair, *Infrared Spectroscopy in Surface Chemistry* (Marcel Dekker, New York, 1967).
13. A. C. Yang and C. W. Garland, *J. Phys. Chem.* **61**, 1504 (1957).
14. C. W. Garland, R. C. Lord, and P. F. Troiano, *J. Phys. Chem.* **69**, 1188 (1965).
15. H. Arai and H. Tominaga, *J. Catalysis* **43**, 131 (1976).
16. D. J. C. Yates, Conference on Catalyst Deactivation and Poisoning, May 24-28, 1978, Lawrence Berkeley Laboratory, Berkeley, Calif. 94720, Pub. 238.



17. H. C. Yao and W. G. Rothschild, J. Chem. Phys. 68, 4774 (1978).
18. L. F. Dahl, C. Martell, and D. L. Wampler, J. Amer. Chem. Soc. 83, 1761 (1961).
19. C. W. Garland and J. R. Wilt, J. Chem. Phys. 36, 1094 (1962).
20. Obtainable from the Harshaw Chemical Company, Crystal and Electronic Products Department, 6801 Cochran Road, Solon, Ohio 44139.
21. Alon C is a high-area alumina supplied by Godfrey L. Cabot, Inc., Boston, Massachusetts 02110. The specific surface area of this lot, produced in 1958, is  $90 \text{ m}^2 \text{g}^{-1}$ .
22. E. K. Plyler, A. Danti, L. R. Blaine, and E. D. Tidwell, J. Res. N.B.S., A, 64, 29 (1960).
23. E. S. Ebers and H. H. Nielsen, J. Chem. Phys. 6, 311 (1938).
24. B. A. Sexton and G. A. Somorjai, J. Catalysis 46, 167 (1977).
25. E. R. Corey, L. F. Dahl, and W. Beck, J. Amer. Chem. Soc. 85, 1202 (1963).
26. G. Bor, J. Organometallic Chemistry 10, 343 (1967).
27. S. F. A. Kettle and I. Paul, Advances in Organometallic Chemistry 10, 199 (1972).
28. J. Dalton, I. Paul, and F. G. A. Stone, J. Chem. Soc. A, 2744 (1969).

TABLE I

Comparison of Full-Coverage Infrared Spectrum of CO on Rh/Al<sub>2</sub>O<sub>3</sub> at 300 K

<u>%Rh/Al<sub>2</sub>O<sub>3</sub></u>	<u>Rh-CO</u>	<u>Species (<math>\tilde{\nu}</math>) - (cm<sup>-1</sup>)</u>		<u>Reference</u>
		<u>Rh(CO)<sub>2</sub></u>	<u>Rh<sub>2</sub>(CO)</u>	
2.2%	2070	2101 ; 2031	1870	This work
2.0%	~2068	2095 ; 2027	--	(13)
0.92%	~2069	2100 ; 2030	1850	(17)
?	Unresolved	2108 ; 2040	1360	(15)



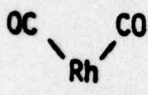
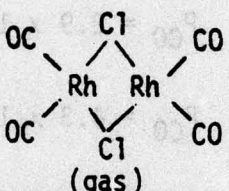
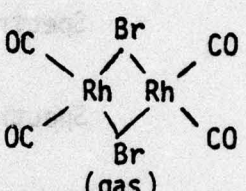
TABLE II

Comparison of Full-Coverage  $^{12}\text{CO}$  and  $^{13}\text{CO}$  Stretching Frequencies on  $\text{Rh}/\text{Al}_2\text{O}_3$

	<u>Species (<math>\tilde{\nu}</math>) - (<math>\text{cm}^{-1}</math>)</u>		
	<u>Rh-CO</u>	<u>Rh(CO)<sub>2</sub></u>	<u>Rh<sub>2</sub>(CO)</u>
$^{12}\text{CO}$	2070	2101;2031	1870
$^{13}\text{CO}$	2024	2056;1987	1832
$\Delta\tilde{\nu}$	46	45;44	38
$\Delta\tilde{\nu}_{\text{calc.}}$	46	47;45	42

TABLE III

Comparison of Symmetric and Antisymmetric  
Carbonyl Stretching Frequencies

	<u>Species</u>		
	 $\text{Al}_2\text{O}_3$ $(\text{cm}^{-1})$	 $(\text{gas})$ $(\text{cm}^{-1})$	 $(\text{gas})$ $(\text{cm}^{-1})$
$\tilde{\nu}_{\text{sym}}$	2101	2095	2092
$\tilde{\nu}_{\text{asym}}$	2031	2043	2042
Reference:	this work	(19)	(19)



### Figure Captions

Figure 1. Side view of vacuum cell used for transmission infrared spectroscopy through supported metals.

Figure 2. Typical isotherm for CO chemisorption on supported Rh.  $T = 295$  K.  
(The labeled points correspond to spectra shown in Figure 3.)

Figure 3. Infrared spectra for  $^{12}\text{CO}$  adsorbed on Rh for increasing CO coverage.  
 $T = 295$  K.

Spectrum (a).  $P_{\text{CO}} = 2.9 \times 10^{-3}$  torr

Spectrum (b).  $P_{\text{CO}} = 4.3 \times 10^{-3}$  torr.

Spectrum (c).  $P_{\text{CO}} = 5.0 \times 10^{-3}$  torr.

Spectrum (d).  $P_{\text{CO}} = 8.3 \times 10^{-3}$  torr.

Spectrum (e).  $P_{\text{CO}} = 0.76$  torr.

Spectrum (f).  $P_{\text{CO}} = 9.4$  torr.

Spectrum (g).  $P_{\text{CO}} = 50$  torr.

Figure 4. Infrared spectra for  $^{12}\text{CO}$  on Rh following desorption.

Spectrum (a). Full coverage at  $\sim 50$  torr,  $295$  K.

Spectrum (b). Desorption time,  $150$  s,  $295$  K.

Spectrum (c). Desorption time,  $3.6 \times 10^4$  s,  $321$  K.

Spectrum (d). Desorption time,  $2.2 \times 10^4$  s,  $336$  K.

Figure 5. Infrared spectra for 90%- $^{13}\text{C}$ O adsorbed on Rh for increasing CO coverage  
 $T = 295 \text{ K}$ .

Spectrum (a).  $P_{\text{CO}} = 7 \times 10^{-3} \text{ torr}$ .

Spectrum (b).  $P_{\text{CO}} = 7 \times 10^{-3} \text{ torr}$ .

Spectrum (c).  $P_{\text{CO}} = 7.5 \text{ torr}$ .

Spectrum (d).  $P_{\text{CO}} \approx 50 \text{ torr}$ .

Figure 6. Spectral changes during isotopic exchange of  $^{13}\text{C}$ O(ads) with  $^{12}\text{C}$ O(g).  
 $T = 295 \text{ K}$ .

Spectrum (a). Full coverage  $^{13}\text{C}$ O (90%) achieved at  $\sim 50 \text{ torr}$ .

Spectrum (b). Following 660 sec. exchange with  $^{12}\text{C}$ O at 50 torr.



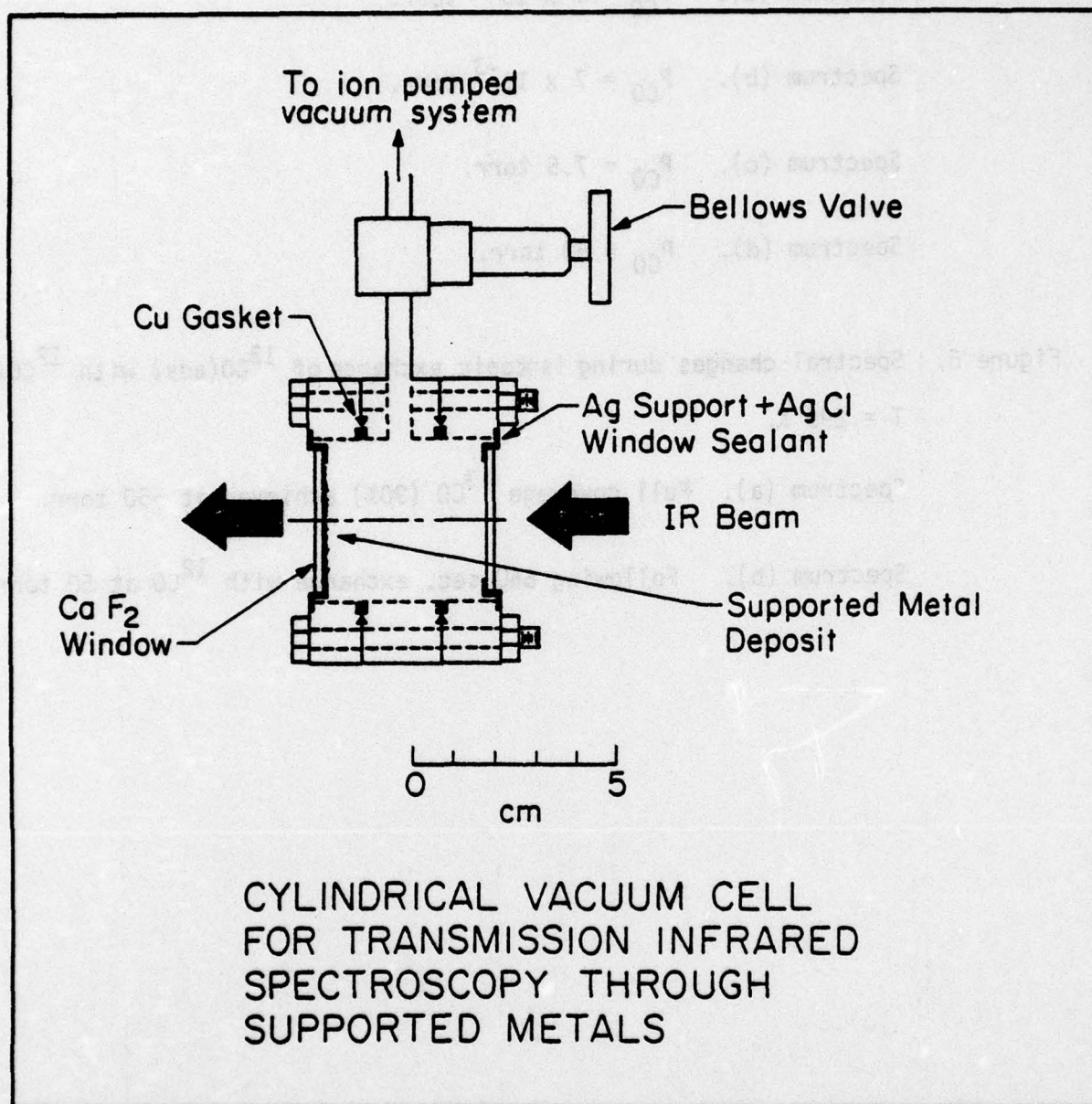


Figure 1

TYPICAL ISOTHERM FOR CO  
CHEMISORPTION ON SUPPORTED Rh.  
T=295 K

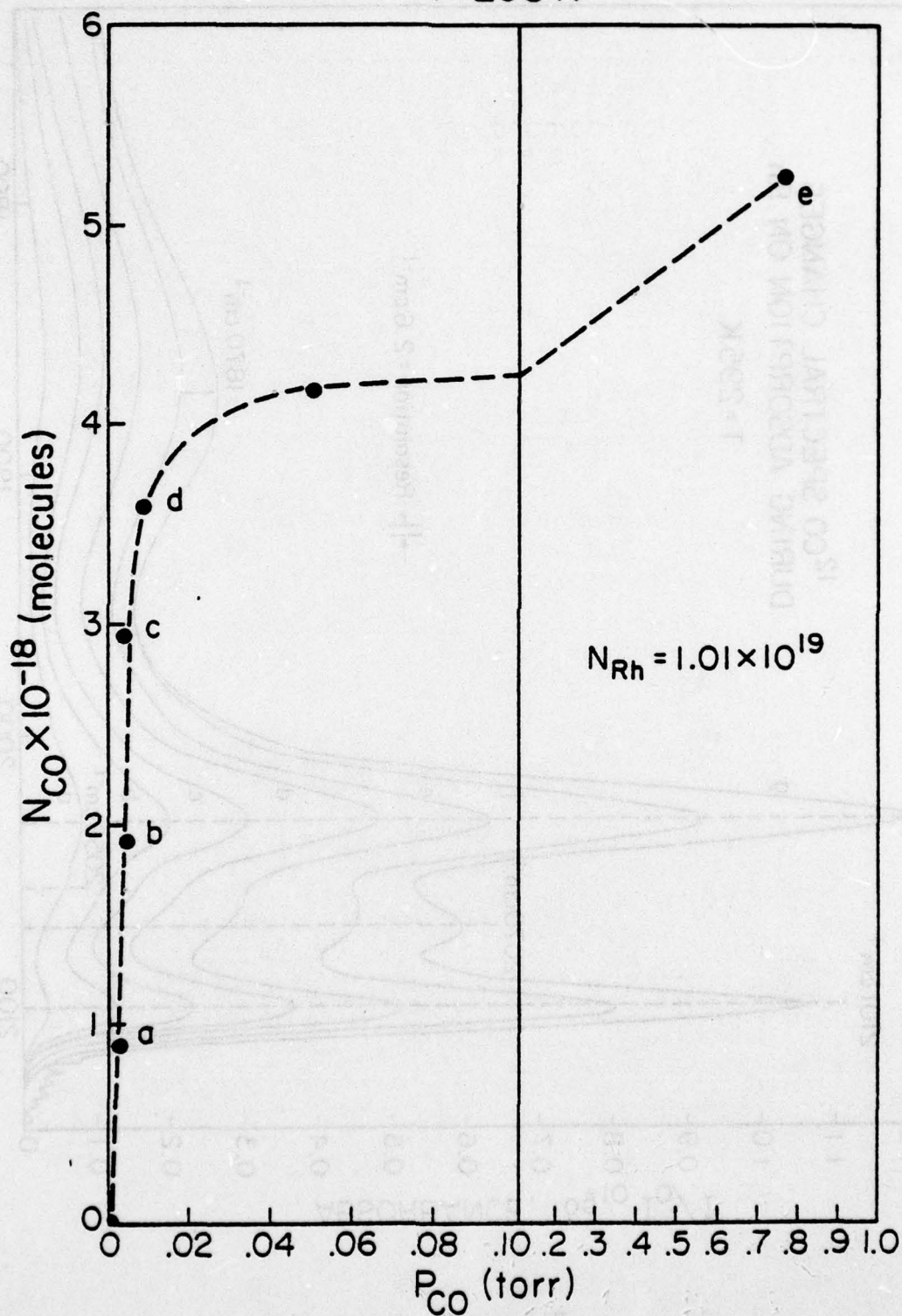


Figure 2



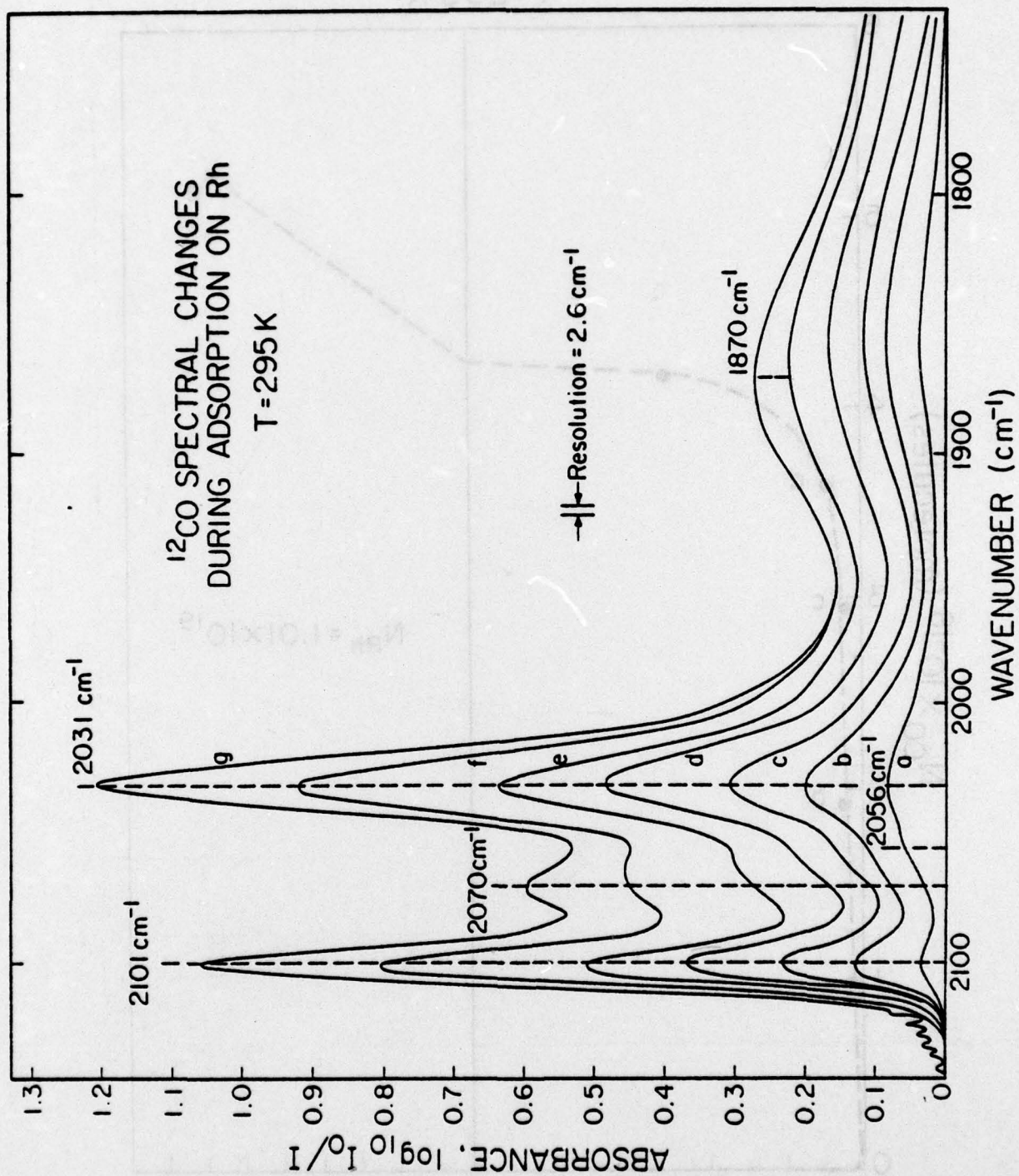


Figure 3

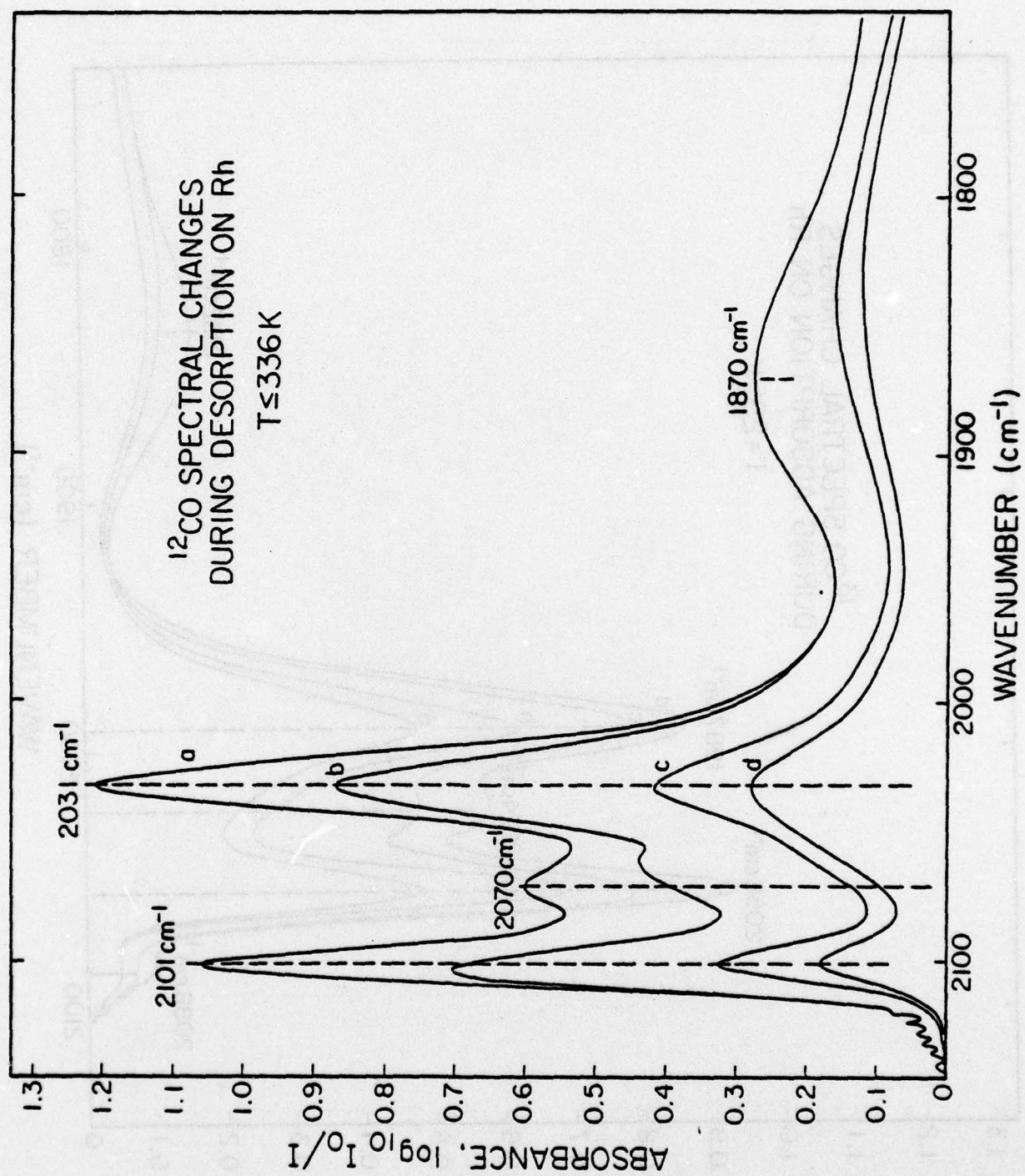


Figure 4



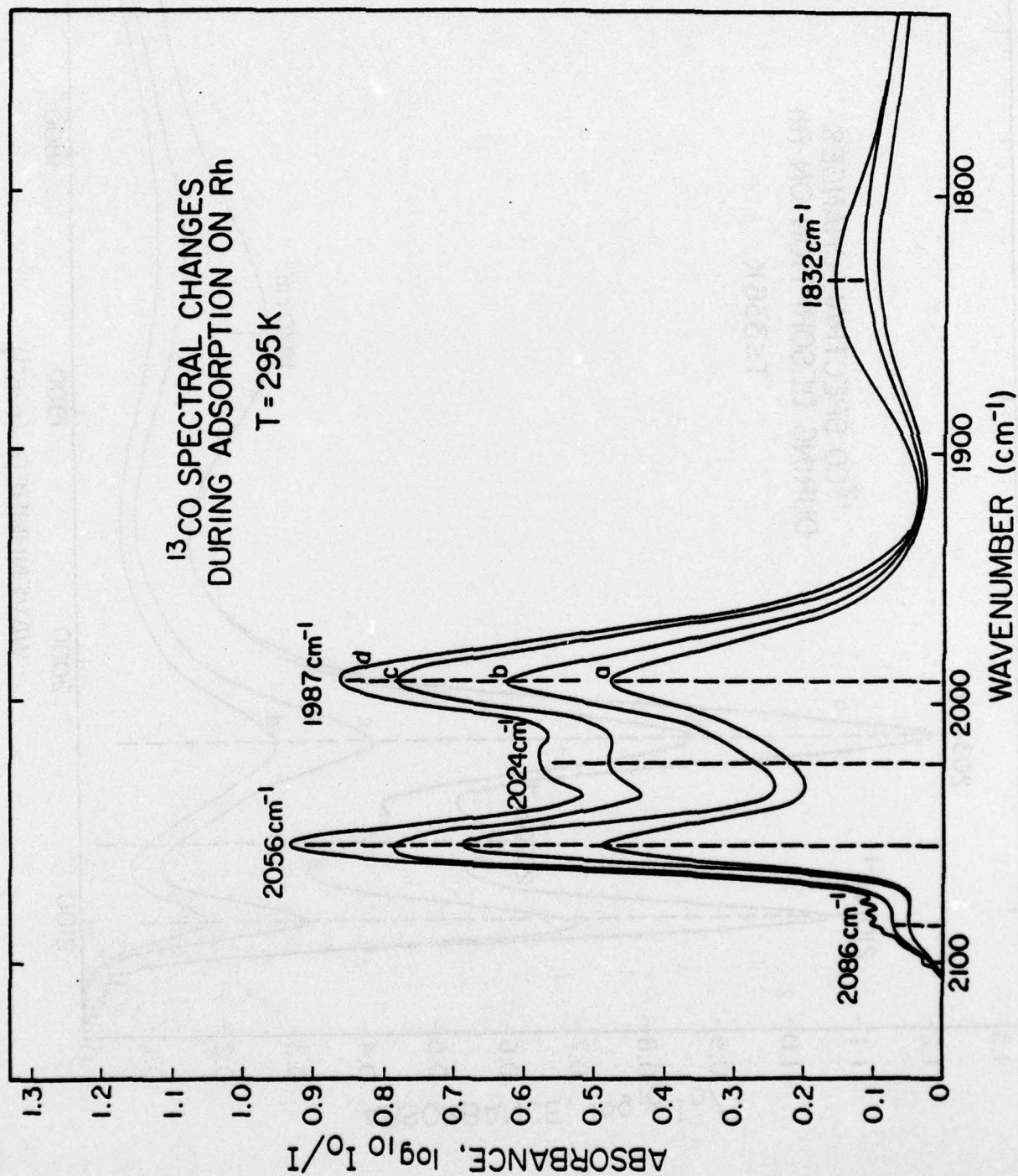


Figure 5

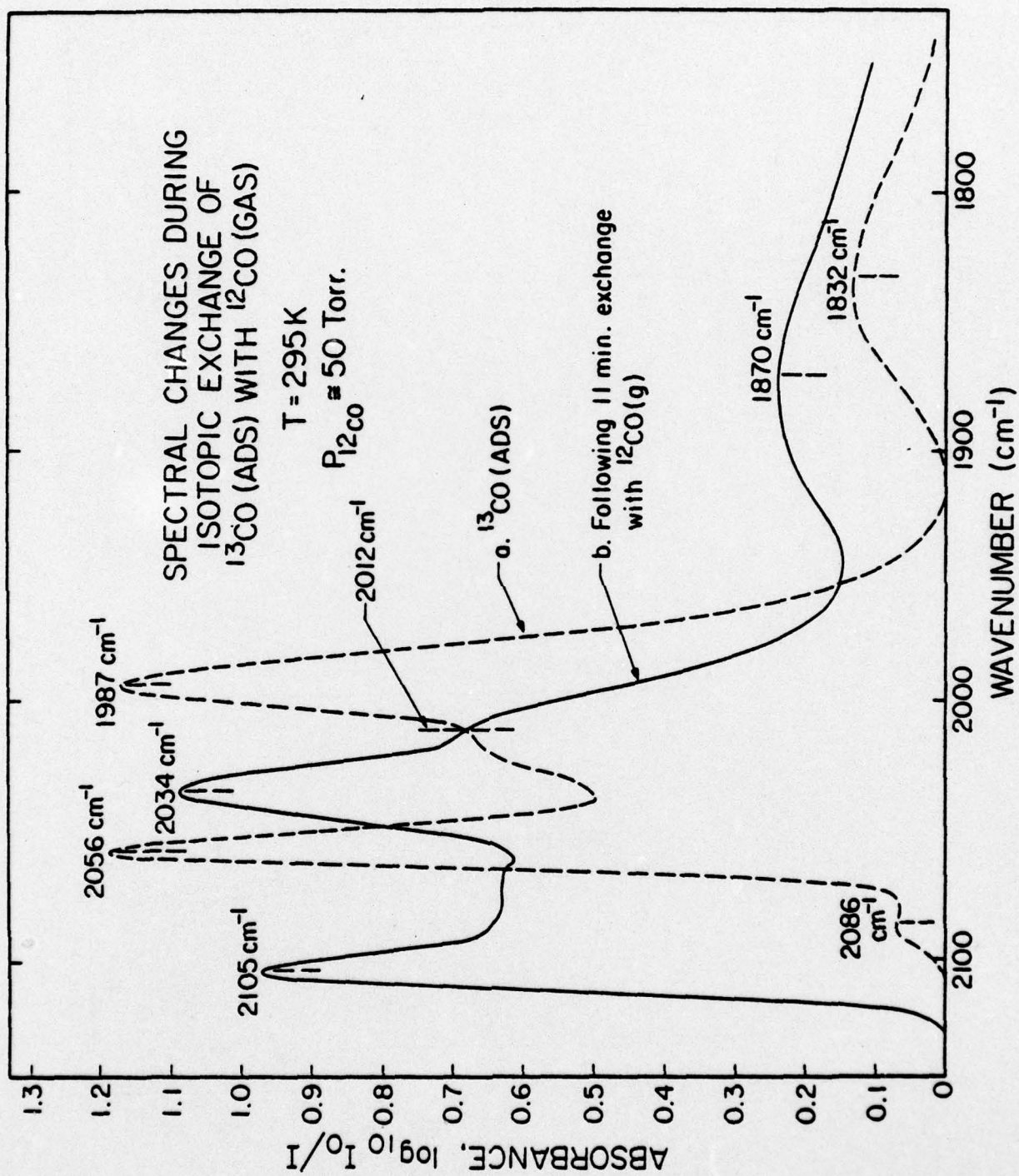


Figure 6